[7]DeBonis, J. R., Georgiadis, N. J., and Smith, C. F., "Validation of the NPARC Code for Nozzle Afterbody Flows at Transonic Speeds," AIAA Paper 95-2614, July 1995.

[8]Lam, D. W., "Use of the PARC Code to Estimate the Off-Design Transonic Performance of an Over/Under Turboramjet Nozzle," AIAA Paper 95-2616, July 1995.

[9]McNally, W. D., "Fortran Program for Calculating Compressible Laminar and Turbulent Boundary-Layers in Arbitrary Pressure Gradients," NASA TN D-5681, May 1970, p. 15.

[10]Back, L. H., Massier, P. F., and Cuffel, R. F., "Flow Phenomena and Convective Heat Transfer in a Conical Supersonic Nozzle," *Journal of Spacecraft and Rockets*, Vol. 4, No. 8, 1967, pp. 1040–1047.

J. C. Hermanson
*Associate Editor*

# Hypersonic Flow Control Using Upstream Focused Energy Deposition

David W. Riggins* and H. F. Nelson†
*University of Missouri–Rolla, Rolla, Missouri 65409-0050*

## Introduction

REDUCTIONS in the drag of hypersonic airplanes is very beneficial, yielding gains in speed and economy of operation. Significant drag reduction for supersonic blunt-nosed bodies is obtained using a structural spike extending forward from the nose.[1] Pressure drag can drop by 50% or more because the blunt body detached normal shock is no longer present. However, usefulness of structural spikes is limited due to cooling requirements and frictional drag. Nonstructural spikes, produced by depositing energy at an upstream point in the flow, may generate similar drag reduction as structural spikes.

The potential of using energy-assisted shaping of high-speed flows has been the subject of several investigations. Bushnell[2] suggested that energy tailoring could produce two benefits: 1) high effective fineness ratios with accompanying drag decrease and 2) sonic boom reduction for supersonic aircraft. Miller and Carlson[3] and Batdorf[4] investigated the possibility of reducing the strength of sonic booms using energy deposition.

Marsh et al.[5] and Toro et al.[6] considered using directed energy to detonate air in front of a vehicle, to form a detached blast wave surrounding the vehicle. The vehicle then flies behind the blast wave shock at a much lower effective Mach number, thereby reducing wave drag.

The Russian literature contains many papers investigating the effect of energy deposition upstream of supersonic and hypersonic blunt bodies. A review of this literature was recently presented.[7] Russian scientists have done numerical studies that show that upstream energy deposition can reduce wave drag for spheres and elliptic-nosed bodies up to 50% or more. They have also shown that it is possible to generate lift and pitching moment by moving the energy deposition point off the centerline. The Russians have also done experiments using electric discharges and lasers to deposit energy into the flow and obtained photographs of the modified shock structure.

Riggins et al.[8] recently presented a numerical study of wave drag reduction using energy deposition at a point on the centerline in front of hypersonic blunt bodies. The energy deposition modified the shock structure and resulted in wave drag reductions of up to 70%.

There is no consensus agreement as to the cause of these changes in wave drag. It may be due mainly to heat addition and the resulting higher temperatures, or it may be due to gasdynamic effects caused by nonequilibrium plasmas. The objective of this study is evaluate the feasibility of using focused energy deposition to modify the flowfield around hypersonic blunt bodies and to reduce wave drag. Energy deposition is considered both on and off the stagnation streamline. Upstream energy deposition results in significant drag reduction. Off-centerline deposition locations are of interest due to modification of both lift and pitching moment. Upstream energy deposition could influence hypersonic vehicle design by 1) requiring smaller propulsion systems, 2) reducing fuel consumption, 3) increasing structural integrity, 4) enabling larger payloads at smaller takeoff gross weight, 5) increasing lift-to-drag ratios, and 6) resulting in new and unique control systems.

## Computational Methodology

This research was done using a modified version of the time-marching Navier–Stokes code SPARK, originally developed by Drummond et al.[9] at NASA Langley Research Center. The full viscous Navier–Stokes equations with variable thermodynamic and diffusion properties and variable specific heats are solved in an explicit time-marching fashion.

Energy deposition in the flow was modeled by modifying the energy equation to include an energy source term. The source term represents the volumetric heating rate, defined as $\dot{Q}/(N\Delta A)$, where $\Delta A$ represents the side area of a grid cell in the deposition volume and $N$ is the number of grid cells in the deposition volume. Typically, $\Delta A$ is rectangular in shape with an axial $x$ length of $h/15$ and a height $z$ of $h/56$, where $h$ is the blunt-body height. It has unit thickness in the $y$ direction, so that $\dot{Q}$ has units of kilowatt per meter.

Convergence of the flowfield solution is determined by monitoring drag of the body. Typically drag reaches its asymptotic limit prior to 20,000 iterations. However, solutions are generally run for 40,000 iterations to ensure convergence. Grid refinement and time convergence are discussed in Refs. 8 and 10.

All calculations assume zero angle of attack and laminar flow with a Prandtl number of 0.7. Air dissociation is not considered. No attempt is made to model the base of the blunt body. The base may be considered to be the aft end of an impulse engine providing the required thrust for the given cruise condition.

## Analysis

The ratio of drag with power deposition to drag with no power deposition is defined[8,10] as

$$R_D = \frac{D_{\text{mod}}}{D_{\text{ref}}} = \frac{D_{\text{mod}} V_\infty}{D_{\text{ref}} V_\infty} \tag{1}$$

where $R_D$ is also equal to the power required for cruise, with energy deposition divided by the power required for cruise with no energy deposition.

Power effectiveness is defined as the ratio of propulsive power saving due to flowfield modification divided by the power required to modify the flowfield[8,10] such that

$$S_D = (D_{\text{ref}} - D_{\text{mod}}) V_\infty / \dot{Q} = (D_{\text{ref}} V_\infty / \dot{Q})(1 - R_D) \tag{2}$$

where $\dot{Q}$ is the energy deposition rate. $S_D$ represents the efficiency of the energy deposition process from a management standpoint. Small values of $R_D$ and large values of $S_D$ are desirable.

Off-centerline energy deposition creates lift and pitching moment. Parameter $S_L$ represents the ratio of lift power created to power deposited in the flowfield:

$$S_L = L_{\text{mod}} V_\infty / \dot{Q} \tag{3}$$

Parameter $S_M$ represents the ratio of pitching moment power created to power deposited in the flowfield:

$$S_M = \frac{M_{\text{mod}} V_\infty}{\dot{Q} h} \tag{4}$$

Presented as Paper 99-0898 at the 37th Aerospace Sciences Meeting, Reno, NV, 11–14 January 1999; received 16 January 1999; revision received 1 September 1999; accepted for publication 3 November 1999. Copyright © 1999 by the American Institute of Aeronautics and Astronautics, Inc. All rights reserved.

*Associate Professor of Aerospace Engineering, Department of Mechanical and Aerospace Engineering and Engineering Mechanics; currently at Department of Aerospace Engineering, University of Tennessee, Knoxville, TN 37996-2210. Senior Member AIAA.

†Professor of Aerospace Engineering, Thermal Radiative Transfer Group, Department of Mechanical and Aerospace Engineering and Engineering Mechanics. Associate Fellow AIAA.

## Results and Discussion

The effect of modifying the flowfield using upstream, focused power addition is investigated for a two-dimensional blunt body flying at Mach 6.5 ($V_\infty = 1981$ m/s) at an altitude of 30 km ($P_\infty = 1185.5$ N/m$^2$, $\rho_\infty = 0.01786$ kg/m$^3$) at zero angle of attack, as shown in Fig. 1. The body has a cylindrical nose, a thickness $h = 0.015$ m, and essentially an infinite length. Calculations were carried out to 0.0165 m behind the stagnation point. Results are presented for a power deposition point located on the stagnation streamline at $x/h = -0.9$ and $z/h = 0$ (0.135 m in front of the stagnation point). Off-axis positions were located at $x/h = -0.9$ and $z/h = 0.1$, 0.2, and 0.3. The power deposition volume is rectangular in shape with an axial length of $h/15$ and a height of $h/56$ centered on the deposition point. The problem is two dimensional; hence, the width can be taken as 1 m.

### Shock Layer Structure

Figure 2 presents pressure and Mach number contours for the blunt body with no energy addition in the flowfield. They are symmetric around the body. The shock standoff distance and shock shape are in good agreement with the predictions of Billig.[11] The pressure is large near the stagnation point and decreases as the flow expands around the shoulder of the body. There is a large subsonic region near the stagnation point that extends well up on the shoulder of the body.

Figure 3 presents pressure and Mach contours for 60 kW/m of energy addition at $x/h = -0.9$ and $z/h = 0.3$. The shock standoff distance and shock shape are complicated functions of position around the nose of the body. An oblique shock forms at the energy deposition point. The flow behind this oblique shock is supersonic, and this leads to a strong shock perpendicular to the body at the body stagnation point. This perpendicular shock is part of the secondary shock system, and it merges with the oblique shock to form the bow shock below the body. There is a large subsonic region near the stagnation point that extends from the normal shock just behind the oblique shock to well up on both the top and bottom shoulders of the body. Embedded in the subsonic region is a small supersonic region located near the shock that is perpendicular to the body. The pressure is large near the body stagnation point and decreases as the flow expands around the top and bottom shoulders of the body. In summary, off-axis energy deposition leads not only to very complicated shock structure and flow patterns but also to production of lift and pitching moment and to reduction of vehicle drag.

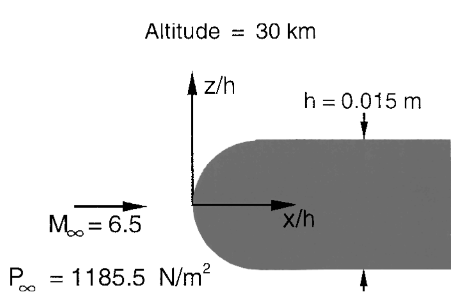


**Fig. 1 Schematic of the hypersonic blunt body.**

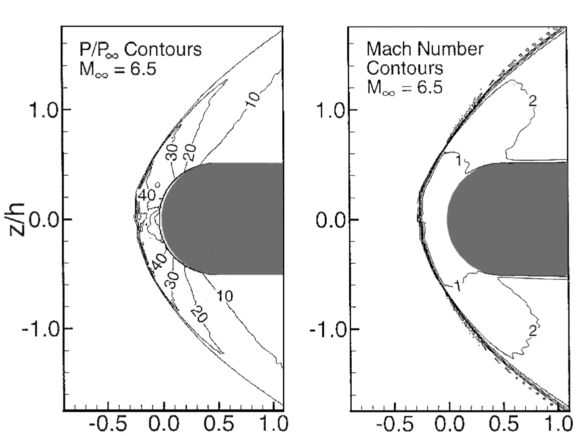


**Fig. 2 Nondimensional pressure and Mach number contours for the reference case.**

**Table 1 Variation of $R_D$ and $S_D$ with $\dot{Q}$, $D_{\text{ref}} = 663$ N/m**

| $\dot{Q}$, kW/m | $\bar{Q}_{\text{NR}}$ | $z/h = 0$ | $z/h = 0.1$ | $z/h = 0.2$ | $z/h = 0.3$ |
|---|---|---|---|---|---|
| | | | $R_D$ | | |
| 0.0 | 0.0000 | 1.00 | 1.00 | 1.00 | 1.00 |
| 4.0 | 0.0038 | 0.830 | 0.906 | 0.928 | 0.951 |
| 20.0 | 0.0192 | 0.536 | 0.748 | 0.814 | 0.897 |
| 40.0 | 0.0384 | 0.474 | 0.725 | 0.774 | 0.909 |
| 60.0 | 0.0576 | 0.448 | 0.695 | 0.775 | 0.889 |
| | | | $S_D$ | | |
| 0.0 | 0.0000 | —— | —— | —— | —— |
| 4.0 | 0.0038 | 55.8 | 30.9 | 23.6 | 16.1 |
| 20.0 | 0.0192 | 30.5 | 16.5 | 12.2 | 6.76 |
| 40.0 | 0.0384 | 17.3 | 9.03 | 7.42 | 2.99 |
| 60.0 | 0.0576 | 12.1 | 6.68 | 4.93 | 2.43 |

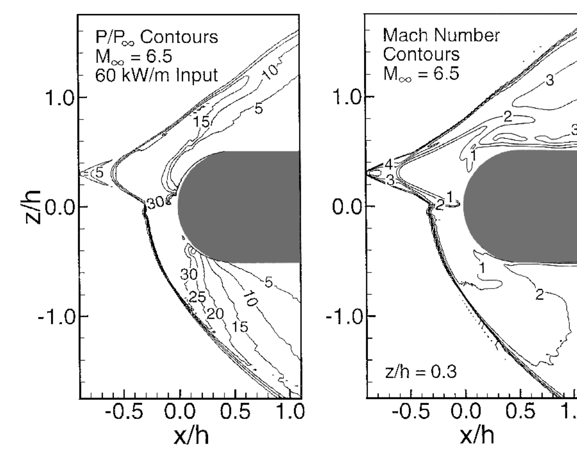


**Fig. 3 Nondimensional pressure and Mach number contours for 60 kW/m deposited at $x/h = -0.9$ and $z/h = 0.3$.**

### Drag Ratio and Effectiveness

The variation of $R_D$ and $S_D$ as a function of the magnitude and position of the power deposited in the flowfield yields further insight into the possible power savings. As the deposit point moves away from the centerline, energy deposition becomes less effective, but even for the least effective case drag is reduced by 10%. $S_D$ is large for low $\dot{Q}$ and drops off as $\dot{Q}$ increases and as the deposition point moves away from the centerline. Table 1 presents values for $R_D$ and $S_D$. Note that $S_D$ is undefined for $\dot{Q} = 0$.

### Lift and Pitching Moment Effectiveness

Recall that $S_L$ is proportional to the ratio of the lift produced to the power deposited. Large values of $S_L$ are desirable. $S_L$ is large for low $\dot{Q}$ and drops off as $\dot{Q}$ increases and as the deposition point moves away from the centerline. Table 2 presents the values of $S_L$ and $S_M$. The values of $S_L$ and $S_M$ are undefined for $\dot{Q} = 0$.

Remember that $S_M$ is proportional to the ratio of pitching moment created to $\dot{Q}$. Both $S_L$ and $S_M$ are large for low $\dot{Q}$ and drop off as $\dot{Q}$ increases and as the input point moves away from the centerline.

### Comparison to Russian Work

The Russians[7,12] presented three-dimensional results for $R_D$ and $S_D$ at Mach 1.5, 3, and 5. The current two-dimensional research is at a higher Mach number, is completely viscous, and applies to a wing leading edge as opposed to the Russian three-dimensional work, which applies to a nose cone. Reference 7 defines a nondimensional power ratio parameter $\bar{Q}_s$ as the ratio of the energy deposition rate to the kinetic energy flux of the freestream intercepted by the body:

$$\bar{Q}_s = \frac{Q_q \rho_\infty V_q}{0.5 \rho_\infty U_\infty^3 \pi R_0^2} \tag{5}$$

**Table 2 Variation of $S_L$ and $S_M$ with $\dot{Q}$**

| $\dot{Q}$, kW/m | $\bar{Q}_{NR}$ | $z/h = 0$ | $z/h = 0.1$ | $z/h = 0.2$ | $z/h = 0.3$ |
|---|---|---|---|---|---|
| | | | $S_L$ | | |
| 0.0 | 0.0000 | —— | —— | —— | —— |
| 4.0 | 0.0038 | 1.86 | 18.0 | 19.1 | 16.6 |
| 20.0 | 0.0192 | 0.163 | 7.18 | 14.0 | 11.1 |
| 40.0 | 0.0384 | 0.063 | 5.67 | 7.40 | 7.18 |
| 60.0 | 0.0576 | 0.00205 | 4.46 | 4.55 | 5.51 |
| | | | $S_M$ | | |
| 0.0 | 0.0000 | —— | —— | —— | —— |
| 4.0 | 0.0038 | 0.993 | 12.0 | 10.8 | 9.16 |
| 20.0 | 0.0192 | 0.0903 | 3.46 | 8.03 | 6.00 |
| 40.0 | 0.0384 | 0.0375 | 2.43 | 3.83 | 3.69 |
| 60.0 | 0.0576 | 0.0123 | 1.95 | 2.33 | 2.80 |

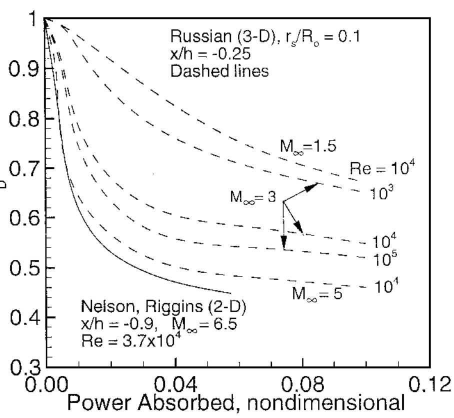


**Fig. 4 Comparison of current and Russian $R_D$ profiles for energy absorbed along centerline (upstream of body at $z/h = 0$).**

where $Q_q$ is the energy deposition rate (watt per kilogram), $U_\infty$ is the freestream velocity (meter per second), $\rho_\infty$ is the freestream density (kilogram per cubic meter), $V_q$ is the cylindrical volume in which the energy is absorbed (cubic meter), and $R_0$ is the radius of the spherical body (meter). The corresponding nondimensional power ratio in the current two-dimensional research is

$$\bar{Q}_{NR} = \dot{Q}/0.5\rho_\infty V_\infty^3 h \tag{6}$$

where values of $\bar{Q}_{NR}$ are given in Tables 1 and 2.

Figure 4 shows a plot of $R_D$ vs either $\bar{Q}_s$ or $\bar{Q}_{NR}$. The Russian data are shown as dashed lines. There are several differences between the flow conditions and geometry of the Russian and current calculations: 1) Russian is three dimensional, current is two dimensional; 2) Russian for $M_\infty = 1.5$, 3, and 5 and three Reynolds numbers, $10^3$, $10^4$, and $10^5$, current for $M_\infty = 6.5$ and $Re = 3.7 \times 10^4$; and 3) Russian and current absorption spot size and position are different. In spite of these differences, the current calculations of $R_D$ have the same trends and magnitude of the previous Russian work. The three-dimensional results allow for pressure reliving and, hence, have slightly less drag reduction, compared to the two-dimensional results.

## Conclusions

This Note presents a parametric study of the effect of energy deposition rate at a point upstream of a hypersonic blunt body on the blunt-body flowfield. It is shown the wave drag is reduced up to 50%, depending on the location of the deposition point. When the deposition point is moved off the stagnation streamline, the energy deposition also produces a lift force and a pitching moment. Trends and magnitudes of the current results are in agreement with recently available Russian results. The modifications in the flowfield created by upstream power deposition may lead to effective ways to stabilize and control hypersonic vehicles.

## Acknowledgments

This research has been partially supported by NASA Grant NAG-1189 from the HYPER-X Program Office, C. R. McClinton, NASA Langley Research Center, Hampton, Virginia, Technical Monitor.

## References

[1] Hutt, C. R., and Howe, A. J., "Forward Facing Spike Effects of Bodies of Different Cross Sections in Supersonic Flow," *Aeronautical Journal of the Royal Aeronautical Society*, Vol. 93, June/July 1989, pp. 229–234.

[2] Bushnell, D. M., "Supersonic Aircraft Drag Reduction," AIAA Paper 90-1596, June 1990.

[3] Miller, D. S., and Carlson, H. W., "A Study of the Application of Heat of Force Field to the Sonic-Boom-Minimization Problem," NASA TND-5582, 1969; also AIAA Paper 70-903, Jan. 1970.

[4] Batdorf, S. B., "On Alleviation of the Sonic Boom by Thermal Means," AIAA Paper 70-1323, 1970.

[5] Marsh, J. J., Myrabo, L. N., Messitt, D. G., Nagamatsu, H. T., and Raizer, Y. P., "Experimental Investigation of the Hypersonic 'Air Spike' Inlet at Mach 10," AIAA Paper 96-0721, Jan. 1996.

[6] Toro, P. G. P., Myrabo, L. N., and Nagamatsu, H. T., "Pressure Investigation of the Hypersonic 'Directed-Energy Air Spike' Inlet at Mach Number 10 with Arc Power up to 70 kW," AIAA Paper 98-0991, Jan. 1998.

[7] Levin, V. A., Afonina, N. E., Gromov, V. G., Georgievsky, P. Y., and Terentjeva, L. V., "Influence of Energy Input by Electric Discharge on Supersonic Flows Around Bodies," *2nd Weakly Ionized Gases Workshop—Proceedings*, 1998, pp. 202–250.

[8] Riggins, D. W., Nelson, H. F., and Johnson, E., "Blunt Body Wave Drag Reduction Using Focused Energy Deposition," *AIAA Journal*, Vol. 37, No. 4, 1999, pp. 460–467.

[9] Drummond, J. P., Rogers, R. C., and Hussaini, M. Y., "A Detailed Numerical Model of a Supersonic Reacting Mixing Layer," AIAA Paper 86-1427, June 1986.

[10] Riggins, D. W., and Nelson, H. F., "Hypersonic Flow Control Using Upstream Focused Energy Deposition," AIAA Paper 99-0898, Jan. 1999.

[11] Billig, F. S., "Shock-Wave Shapes Around Spherical and Cylindrical-Nosed Bodies," *Journal of Spacecraft and Rockets*, Vol. 4, No. 6, 1967, pp. 822–823.

[12] Chernyi, G. G., "The Impact of Electromagnetic Energy Addition to Air near the Flying Body on Its Aerodynamic Characteristics," *2nd Weakly Ionized Gases Workshop—Proceedings*, 1998, pp. 1–32.

M. Samimy
*Associate Editor*

# Ablative Laser Propulsion: An Old Concept Revisited

Andrew V. Pakhomov* and Don A. Gregory†
*University of Alabama in Huntsville,*
*Huntsville, Alabama 35899*

## Introduction

THE concept of laser propulsion (LP) is not very new. The idea was introduced in 1972 by Kantrowitz,[1] passed through a decade of active research in the mid-1970s and mid-1980s, and culminated in the first field demonstrations led by Mead and Myrabo in the mid-1990s.[2–4] The intrigue of the concept is that a vehicle driven by LP needs no engine or fuel in the traditional sense, a major advantage over any rocket, with a promise of a reduction in payload costs down to \$100/kg (compared to \$10,000+ for a modern rocket).[4]

The decade of intensive research in LP was limited to powerful lasers available at the time: mostly $CO_2$ or sometimes hydrogen fluoride–deuterium fluoride (HF-DF). To some extent, the concept was formally divided along two branches defined by the type of laser irradiation: continuous wave (CW) or repetitively pulsed (RP).[3] Research in the steady-state regime (CW) concentrated on describing laser-supported combustion waves (LSC) at low fluences and laser-supported detonation waves (LSD) at higher fluences.[2,3] All momentum transfer in the CW regime occurred through the gaseous or plasma state so that the choice of fluids as propellants for CW propulsion was predetermined.

Received 20 June 1999; revision received 1 December 1999; accepted for publication 14 December 1999. Copyright © 2000 by the American Institute of Aeronautics and Astronautics, Inc. All rights reserved.

*Assistant Professor, Department of Physics.
†Associate Professor, Department of Physics.